Structural Properties of Several Amphiphile Cyclodextrins and Some Related Nanospheres. An X-ray Scattering and Freeze-Fracture Electron Microscopy Study

ARTICLE *in* LANGMUIR · JANUARY 1998

Impact Factor: 4.46 · DOI: 10.1021/la971019r

4 AUTHORS, INCLUDING:

Hervé Delacroix
Université Paris-Sud 11
62 PUBLICATIONS **2,021** CITATIONS
SEE PROFILE

Denis Wouessidjewe
University Grenoble Alpes, Faculty of Pharmacy
82 PUBLICATIONS **1,851** CITATIONS
SEE PROFILE

Mohamed Skiba
Université de Rouen
96 PUBLICATIONS **877** CITATIONS
SEE PROFILE

Structural Properties of Several Amphiphile Cyclodextrins and Some Related Nanospheres. An X-ray Scattering and Freeze-Fracture Electron Microscopy Study

Annette Gulik,*,† Hervé Delacroix,† Denis Wouessidjewe,‡ and Mohamed Skiba‡

Centre de Génétique Moléculaire, CNRS UPR 9061, 91198 Gif sur Yvette Cedex, France, and Laboratoire de Physico-Chimie, Pharmacotechnie et Biopharmacie, CNRS URA 1218, Centre Pharmaceutique, Université Paris XI, rue Jean Baptiste Clément, 92290 Chatenay-Malabry, France

Received September 8, 1997. In Final Form: November 21, 1997

Amphiphilic cyclodextrins bearing fatty acyl chains covalently linked to their secondary hydroxyl groups are able to form nanospheres with an internal organization. The structure of several cyclodextrins with different acyl chain lengths (CD-C*n*) was investigated using X-ray scattering and freeze fracture electron microscopy. From the experimental data and using physicochemical arguments, we propose structure models. βCD-C6, βCD-C8, βCD-C10, βCD-C12, and γCD-C14 form polar columns, surrounded by the paraffin chains, and associated in a 2-D hexagonal lattice. The structure of αCD-C14 and βCD-C14 is body-centered cubic; it comprises one lattice of dimers aligned along the edges of the cubic cell and a second identical lattice with a translation of the half in the three directions. This results in the formation of two globules, one at the apex and one at the center of the cell. The structures are unusual for cyclodextrin molecules; they result from the presence of the numerous paraffin chains linked to each molecule. Indeed, the structures are reminiscent of those found in lipid systems.

Introduction

Natural cyclodextrins (CDs), also named cyclomaltooligosaccharides, are the products of starch bioconversion. They are truncated-cone-shaped molecules, made up of different numbers of a-(1,4) linked D-glucopyranose units in a chair conformation. α-, β-, and γ-cyclodextrins contain six, seven, and eight of such glucose units, respectively. The hydroxyl groups located on the narrowest side and on the widest side of the truncated cone confer a high external hydrophilicity to the molecule. The inside of the cavity with the glucosidic groups is lipophilic. A wide variety of organic molecules of suitable steric hindrance can enter the cavity resulting in an inclusion compound with new physicochemical characteristics. For this reason, cyclodextrins have been proposed for many uses in various industries.[1]

Natural cyclodextrins have been chemically modified to enhance their hydrophilic and lipophilic properties. The frequent starting points for structural modification are hydroxyl groups located on the C2, C3, and C6 of the glucopyranosyl units.[2,3] Cyclodextrin diesters obtained by grafting acyl chains on the secondary hydroxyl functions of glucose units (Figure 1) have been described.[4] A large number of amphiphilic cyclodextrins do not form liposomes in aqueous media but can form stable supramolecular assemblies such as nanospheres. A colloidal dispersion is obtained by mixing an amphiphilic cyclodextrin in solution in acetone with water. The solvent is subsequently removed by evaporation under vacuum, and stable nanospheres are formed.[5] These nanospheres have been characterized and visualized by freeze fracture electron microscopy.[6] The interior of these nanoobjects is undoubtely filled with material that seemed to present some internal organization, although this has not yet been confirmed by X-ray scattering analysis. These preliminary results prompted us to analyze the structural properties of several amphiphilic cyclodextrins, using two complementary approaches, X-ray scattering and freeze-fracture electron microscopy. The present paper describes the self-assembly structural properties of amphiphilic CD and the internal organization of the CD nanospheres.

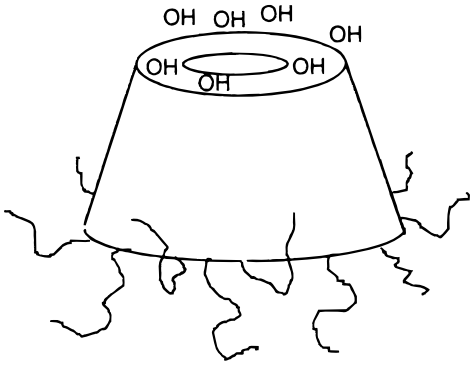

Figure 1. Schematic representation of an amphiphilic cyclodextrin molecule.

* Author for correspondence: tel, 33-(0)169823166; fax, 33-(0)-169823150; e-mail, agulik@cgm.cnrs-gif.fr.

† Centre de Génétique Moléculaire, CNRS UPR 9061.

‡ Université Paris XI.

(1) Duchêne, D.; Wouessidjewe D. Industrial uses of cyclodextrins and their derivatives. *J. Coord. Chem.* **1992**, *27*, 223−236.

(2) Croft, A.-P.; Bartsch, R.-A. Synthesis of chemically modified cyclodextrins. *Tetrahedron* **1983**, *39*, 1417−1474.

(3) Wenz, G. Cyclodextrins as building blocks for supramolecular structures and functional units. *Angew. Chem., Int. Ed. Engl.* **1994**, *33*, 803−822.

(4) Zhang, P.; Ling, C.-C.; Coleman, A.-W.; Parot-Lopez, H.; Galons, H. Formation of amphiphilic cyclodextrins via esterification at the secondary hydroxyl face. *Tetrahedron Lett.* **1991**, *32*, 2769−2770.

(5) Skiba, M.; Duchêne, D.; Puisieux, F.; Wouessidjewe, D. Development of a new drug carrier from chemically modified cyclodextrins: nanospheres and the influence of physicochemical and technological factors on particle size. *Int. J. Pharm.* **1996**, *a129*, 113−121.

(6) Skiba, M.; Wouessidjewe, D.; Puisieux, F.; Duchêne, D.; Gulik, A. Characterization of amphiphilic β-cyclodextrin nanospheres *Int. J. Pharm.* **1996**, *b142*, 121−124.

S0743-7463(97)01019-6 CCC: $15.00
Published on Web 01/30/1998

Table 1[a]

	100%			90%	
compound	V_{pol}	V_{par}	V_{tot}	V_{par}	V_{tot}
αCD-C14	1464	4536	6000	4082	5546
βCD-C6	1638	2268	3906	2041	3679
βCD-C8	1638	3084	4722	2776	4414
βCD-C10	1638	3780	5414	3402	5040
βCD-C12	1638	4536	6176	4082	5720
βCD-C14	1638	5292	6930	4763	6401
γCD-C14	1872	6048	7920	5443	7395

[a] The molecular parameters were determined assuming that 100 or 90% of the secondary hydroxyl groups were esterified with a fatty acid. V_{par} is the hydrocarbon part of the molecule. The calculation of the volume from the chemical parameter was done from the following evaluation: for the polar part (V_{pol}), sugar residue $V \approx 170$ Å^3; COO $V \approx 35$ Å^3; for the paraffinic moiety (V_{par}), CH_3 $V = 54$ Å^3; CH_2 $V = 27$ Å^3.

Material and Methods

Preparation. The compounds were synthesized as described previously.[4]

Nomenclature. CD-C*n* represents a cyclodextrin esterified by an aliphatic carboxylic acid of *n* carbon atoms. α-, β-, and γ-CD define the type of cyclodextrin having six, seven, and eight glycosidic residues, respectively.

Chemical Parameters. We considered the amphiphilic cyclodextrin molecules in two parts: the hydrophobic part composed of the aliphatic chains comprising the hydrocarbon residues and the polar part made of the rest of the molecule. As the esterification may be incomplete, we assumed that on average 90% of the secondary hydroxyl groups were esterified. The molecular parameters adopted are listed in Table 1. V, V_{pol}, and V_{par} are the total, polar, and paraffinic volumes; C_{vpol} and C_{vpar} are the volume concentration of the paraffin and polar moieties. In the absence of water or in the presence of few associated water molecules, the concentrations of the polar and paraffinic parts C_{vpol} and C_{vpar} were estimated to V_{pol}/V and V_{par}/V, respectively.

X-ray Scattering Experiments. The experiments were performed with a focusing Guinier camera, using monochromatic Cu Kα_1 radiation ($\lambda = 1.54$ Å) and linear collimation. Positions in reciprocal space are specified by the parameter $s = 2 \sin \theta/\lambda$, where 2θ is the scattering angle and λ is the wavelength. The films were scanned with a Joyce-Loebel microdensitometer, and the intensities were then measured.

Freeze Fracture Electron Microscopy. Image Analysis and Processing. The samples either dry or dispersed in water or mixed with a small quantity of a hydrophobic solvent (when necessary) were deposited on a copper planchett and quickly frozen in liquid propane, fractured, and shadowed in a Balzers freeze-etch unit using Pt−C or W−Ta shadowing. The replicas were washed with an organic solvent and examined in a Philips 301 electron microscope.

The micrographs revealed the presence of flat fracture surfaces displaying either 1-D or 2-D ordered domains. These periodicities were first characterized by optical diffraction. An area of the replica displaying a 1-D or a 2-D periodic order and whose lattice corresponded to a planar section of the frozen sample normal to the crystallographic direction [*hk*] or [*hkl*] is called [*hk*] or [*hkl*] domain, respectively. The crystallographic orientation is determined with the help of the X-ray scattering information. We call **v** and **w** and γ the vectors and the angle of the 2-D lattice. The periodic domains are usually made of successive levels of fracture within the sample, called subdomains. The subdomains have the same crystallographic orientation and are related to one another by well-defined geometrical operations that depend on the crystallographic space group. The analysis of the electron micrographs was performed on fracture planes parallel to the image planes after inspection of stereoviews. For the 2-D ordered domains, a few selected images were digitized and the cell parameters determined by Fourier transformation. The fracture domains were processed by Fourier filtering in order to enhance the contrast of the periodic information. These filtered images were then inspected to identify the different fracture aspects within a domain as well as the boundaries of the corresponding different subdomains. For each aspect, a subdomain was Fourier-filtered using the previously determined cell parameters. A fragment of the filtered image of a subdomain was then cross-correlated with the image of the whole fracture domain. From the relative correlation map, the relationships between equivalent subdomains were analyzed and an averaged motif of the periodic content of each class of subdomains was obtained by the cross-correlation averaging technique.[7,8]

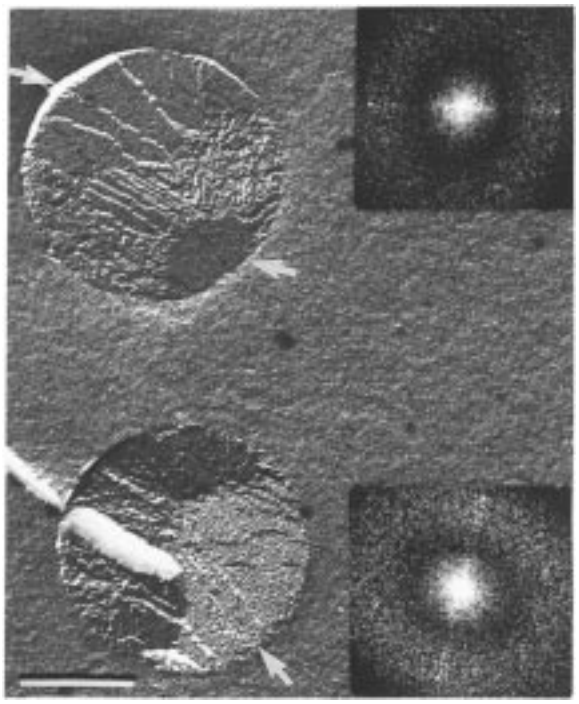

Figure 2. Freeze fracture electron microscopy of a βCD-C14 nanosphere dispersion. 2D ordered fracture planes can be observed (arrows); insert: optical diffraction of the ordered domains. Bar = 200 nm.

Results

Preliminary X-ray scattering spectra of centrifuged nanospheres of βCD-C6, βCD-C12, and βCD-C14 were typical of liquid crystalline phases: for βCD-C6 and βCD-C12, three slightly broad reflections in the spacing ratio $1/\sqrt{3}/\sqrt{4}$ compatible with a 2-D hexagonal structure were obtained; for βCD-C14, there were five reflections in the spacing ratio $1/\sqrt{2}/\sqrt{3}/\sqrt{4}/\sqrt{5}$, possibly corresponding to a centered cubic structure. The nonamorphous nature of the nanospheres was confirmed by freeze fracture electron microscopy experiments which revealed ordered fracture planes (Figure 2). However the size of the nanospheres did not allow a thorough analysis of these planes. Since the nanospheres consist of amphiphilic cyclodextrins possibly mixed with some amount of water, the structural study was further performed directly on the synthesized cyclodextrin component, in the presence or in the absence of water.

We investigated the structural properties of cyclodextrins esterified with aliphatic acids of chain length C6 to C14. The following compounds were studied: βCD-C6, βCD-C8, βCD-C10, βCD-C12, βCD-C14, αCD-C14, and γCD-C14.

βCD-C6 had the appearance of a crystalline powder. The longer the chains, the softer the compounds were.

(7) Frank, J.; Goldfarb, W.; Eisenberg, D.; Baker, T. S. Reconstruction of glutamine synthetase using computer averaging. *Ultramicroscopy* **1978**, *3*, 283−290.

(8) Saxton, W. O.; Frank, J. Motif detection in quantum noise-limited electron micrographs by cross-correlation. *Ultramicroscopy* **1977**, *2*, 219−227.

Table 2. Hexagonal Phase Parameters[a]

compound	a	S	C_{vpol}	R_{pol}	L_{max}	Sch[b]
βCD-C6	25.9	581	0.45	9.1	5.9	29.5 or 27.3
βCD-C8	30.8	821	0.38	10.0	7.8	26.5 or 24.6
βCD-C10	33.0	943	0.33	10.0	9.1	26.5 or 24.6
βCD-C12	35.3	1079	0.29	10.0	10.4	26.5 or 24.6
γCD-C14*	37.6	1224	0.28	10.4	11.3	27.6 or 25.6

[a] All the experiments were performed at room temperature, (*) except for γCD-C14 (47 °C). a (Å) is the lattice cell dimension. S (Å^2) is the surface area of the 2D hexagonal lattice $S = a^2\sqrt{3}/2$. R_{pol} (Å) is the polar radius of the transverse section of the hexagonal cell. $R_{pol} = a(\sqrt{3}c_{vpol}/2\pi)^{1/2}$. In the absence of water $Cv_{pol} = V_{pol}/V_{tot}$. L_{max} (Å) corresponds to the largest distance from the center of the paraffinic medium of the 2-D hexagonal cell to the polar interface $L_{max} = a/\sqrt{3}R_{pol}$. [b] The two values correspond to 90 or 100% of esterification of the secondary hydroxyl groups.

βCD-C6, -C8, -C10, and -C12 and γCD-C14 were optically birefringent. βCD-C14 and αCD-C14 were optically isotropic.

X-ray Diffraction Studies. The compounds were first studied in the absence of added water. They all gave a series of sharp reflections that could be indexed either in a two-dimensional hexagonal lattice or in a three-dimensional cubic lattice. No significant difference was observed in excess water, except that the lattice dimensions were increased by about 1 to 1.5% in most cases and about 3% for βCD-C6. In all cases, a diffusion band was also observed around 4.5 Å, characteristic of the presence of fluid paraffinic chains.

For βCD-C6, βCD-C8, βCD-C10, and βCD-C12, a set of seven sharp reflections in the spacing ratio $1/\sqrt{3}/\sqrt{4}/\sqrt{7}/\sqrt{9}/\sqrt{12}/\sqrt{13}$ was observed; these reflections were consistent with a two-dimensional hexagonal lattice of dimension 25.9, 30.8, 33.0 and 35.3 Å for βCD-C6, βCD-C8, βCD-C10, and βCD-C12, respectively. For βCD-C12, the reflections were slightly less thin. As the lattice dimensions vary according to the length of the paraffin chains, it is probable that the elements of the lattice consist of columns separated by the paraffinic medium. The surface area varied almost linearly as a function of the inverse of the polar volumic content ($1/C_{vpol}$). Consequently, the calculated polar radius is almost constant (Table 2).

The small-angle X-ray scattering pattern of γCD-C14 at room temperature exhibited only a broad band and no sharp reflection. Samples heated to 47 °C gave reflections with spacings in the ratio $1/\sqrt{3}/\sqrt{4}/\sqrt{7}/\sqrt{9}$ that correspond to a 2-D hexagonal lattice with a cell parameter $a = 37.6$ Å (Table 2).

The βCD-Cn class with an acyl chain length of 14 carbon atoms long (βCD-C14) showed a cubic phase but no hexagonal phase. The X-ray diffraction pattern displayed a series of sharp reflections in the spacing ratio $1/\sqrt{2}/\sqrt{3}/\sqrt{4}/\sqrt{5}/\sqrt{6}/\sqrt{7}$. As the material was optically isotropic, it may thus be considered that the lattice is cubic. Since $1/\sqrt{7}$ is not compatible with a cubic lattice, the spacing ratio of the reflections is $\sqrt{2}/\sqrt{4}/\sqrt{6}/\sqrt{8}/\sqrt{10}/\sqrt{12}/\sqrt{14}$. The observed reflections can be thus identified as (110), (200), (211), (220), (310), (222), and (321). As these reflections (hkl) follow the selecting rule, "$h + k + l = 2n$", they clearly identify a body-centered cubic lattice. For βCD-C14, the cubic cell dimension was $a = 43.0$ Å.

αCD-C14 also exhibited the same set of reflections, the spacings of which gave almost the same cubic lattice dimension, $a = 42.6$ Å.

Freeze Fracture Electron Microscopy. We also investigated the structural properties of the amphiphilic cyclodextrins using freeze fracture electron microscopy. Freeze fracture analysis is a useful and powerful tool to analyze ordered lipid water phases.[9] However, in the present case, two difficulties were encountered. First, the lattice dimensions of the amphiphilic cyclodextrin systems were smaller than those of the amphiphilic systems to which the freeze fracture technique is usually applied and are close to the typical resolution of the technique (1.5 nm). Second, it was difficult to obtain large fracture planes because of the stiffness of the material. This is probably due to the structure and to the chemical composition of the samples: rigidity of the CD moiety, saturation of the paraffinic chains (systems containing saturated paraffinic chains are difficult to preserve during the freezing process), small amount of water within the phases, and size of the CD molecules with respect to the lattice dimensions. As the samples were fractured dry or almost dry, the fracture surfaces often appeared crumbled and irregularly organized as if the samples behaved more like a laminated structure than like an assembly of well-defined structural elements (micelles or rodlike features). However, slight heating or an addition of a small amount of a hydrophobic solvent allowed larger fracture planes to be obtained. We checked that the addition of the solvent, decane or toluene, has no influence on the X-ray scattering spectra, although it induced a small increase (2 to 5%) of the lattice parameter.

Freeze fracture micrographs of βCD-C6, -C8, and −C10 are shown in Figure 3. The images are typical of fractured hexagonal lipid phases. For βCD-C6, a very small fractured area was obtained because of the consistency of the sample. Indeed, the micrographs show large islands of organized material separated by smooth domains. For βCD-C8, the addition of a small quantity of hydrophobic solvent was necessary to obtain ordered, albeit small, fracture domains. For βCD-C10 the fracture planes were slightly larger. The optical diffraction of the micrographs yielded repeat distances within the 1-D ordered domains consistent with the lattice dimension determined by the X-ray scattering experiments.

For βCD-C12, the freeze fracture surfaces did not show any ordered domains. This was probably due to the length of the acyl chain. βCD-C12 appeared to have the longest chain compatible with a hexagonal structure of the βCD-Cn series: the addition of two extra carbon atoms (βCD-C14) resulted in a cubic structure.

For α- and βCD-C14, the micrographs of the freeze fracture replicas revealed two-dimensional ordered fracture domains (Figure 3) that look very similar to those of βCD-C14 nanospheres (Figure 2).

All the identified domains belonged to the same orientation. Due to the limited resolution, only three diffraction spots were observed on the optical diffraction. The computed lattice parameters are consistent with those of a fracture plane normal to the [110] crystallographic direction of a body-centered cubic lattice ($\mathbf{v} = \mathbf{w} = a\sqrt{3}/2$, $\gamma = 109°5$). The Fourier filtering of each [110] domain revealed that the fracture subdomains have two possible aspects which appeared alternatively when passing from one subdomain to the neighboring. The corresponding correlation maps were obtained by using either of the two possible filtered content as a reference: they confirmed that the subdomains contain alternative motifs, and they revealed that two successive subdomains having the same content (same class of subdomains) were related to one another by a displacement of $\mathbf{v}/2 + \mathbf{w}/2$, as expected from

(9) Gulik-Krzywicki, T.; Delacroix, H. Combined use of freeze fracture electron microscopy and X-ray diffraction for the structure determination of three-dimensionally ordered specimens. *Biol. Cell* **1994**, *80*, 193−201.

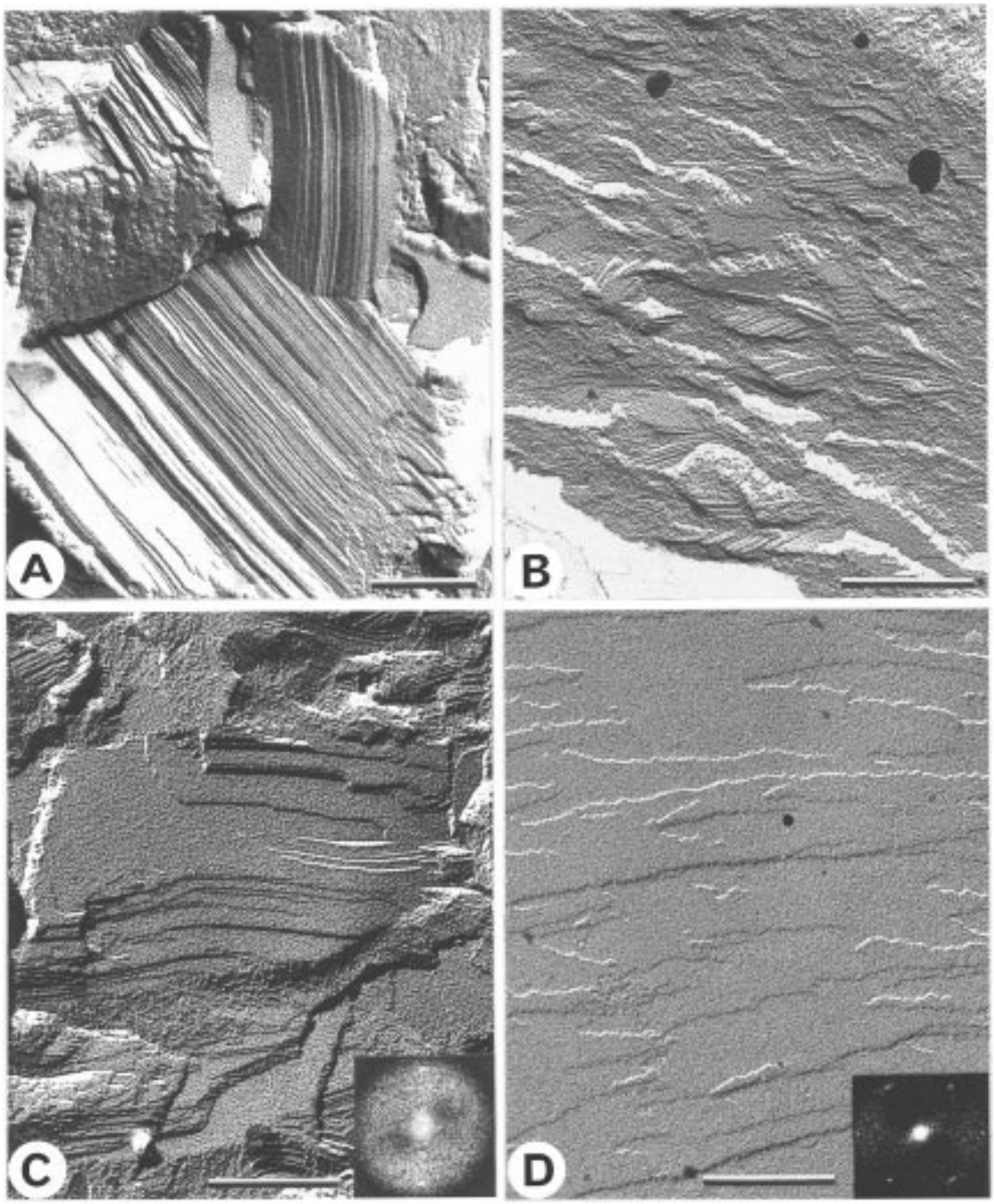

Figure 3. Freeze fracture electron micrographs of β-cyclodextrins: A, CD-C6; B, CD-C8; C, CD-C10 (insert: optical diffraction showing 1-D ordered domains); D, CD-C14 (insert: optical diffraction showing 2-D ordered domains). Bar = 200 nm.

the crystallographic operations of a body-centered cubic structure. The fact that two alternative motifs were observed for the same orientation strongly suggests that the fracture has two possible and "equivalent" pathways through the structure perpendicularly to the [110] axis. The cross-correlation averaging procedure resulted in two different lozenge-like motifs called [110]a and [110]b (Figure 9).

Discussion

The organization of these CD-C*n* compounds bearing aliphatic chains is different from those previously described for cyclodextrins. We will consider the possible arrangements of the amphiphilic cyclodextrin molecules that can account for the existence of the hexagonal or cubic structure. Hexagonal and cubic organizations are common in amphiphilic and lipid−water systems; usually the number of molecules in one unit cell is large and the structure can be solved in terms of a precise spatial distribution of the polar and paraffinic regions.[10] However the relatively small size of the CD-C*n* lattices compared to the size and molecular weight of one molecule indicates that there were few molecules per unit cell. Therefore in the absence of a monocrystal that might yield the determination of the structure at high resolution, the amphiphilic nature of the molecules must be considered to propose a reasonable model for the structure from the

(10) Luzzati, V. X-ray diffraction studies of lipid-water systems. In *Biological Membranes*; Chapman, D., Ed.; Academic Press: New York, 1968; pp 71−123

X-ray powder diffraction and freeze fracture electron microscopy results.

The Hexagonal Structure. Hexagonal packing has already been observed in cyclodextrin crystals, notably by De Rango and co-workers (ref 11 and references therein), particularly those composed of dimers piled in columns parallel to the axis of rotation of the CD molecule. Such columnar assembly is not possible in the present case, since there is about 0.15 molecule in one lattice hexagonal cell of 1 Å thickness (surface area/V_{tot}), that is about one molecule in a height of 5.5 Å (V_{tot}/surface area). Therefore the molecules are necessarily stacked more or less orthogonally to the axis of the columns.

Indeed, the hexagonal structure formed by these molecules is more similar to the structure of lipid or amphiphilic hexagonal phases which can be described as made of quasi-cylindrical columns, parallel to each other and packed according to a two-dimensional hexagonal lattice. This structure belongs to either of two types: in one, H(I), the interior of the cylinder is occupied by the paraffinic moiety and in the other, H(II), it is occupied by the polar part. The position of the hexagonal phase in the lipid water phase diagram and the variation of the lattice with the amount of water generally indicate the type of hexagonal phase.

According to the particular CD geometry and to the large number of paraffin chains per molecule, the number of molecules per unit length in a column is smaller than usual in lipid phases. This restricts the number of spatial arrangements compatible with the data. Given the amphiphilic nature of the molecules we can expect an association of the molecules favoring contact between the hydroxyl headgroups and/or between the paraffinic chains; a paraffin cylinder would impose unlikely associations between the CD moieties inconsistent with their amphiphilic nature. Indeed, the variation of the lattice dimension according to the length of the paraffin chains strongly suggests that the cylinders comprise the polar CD moieties and are separated by a paraffinic matrix: the size of the 2-D surface area of the cell was inversely proportional to the polar volumic content (C_{vpol}), and therefore the corresponding calculated polar radius Rpol of the rod is almost constant (Table 2). Moreover the L_{max} distances (Table 2) between the center of the paraffinic core and the polar interface of the CD moiety cylinder were similar to the distances found in other hexagonal H(II) phases.

Thus the structure consists of polar columns comprising the stacked CD moieties which are surrounded by a paraffinic matrix. If the molecules formed dimers, the packing would be very compact, one dimer every 11 Å. This seems small with respect to the dimension of the small diameter of the truncated cone. Although we cannot rule out this possibility, a more probable arrangement would be made of three molecules in a height of 16.5 Å, a value close to the CD large diameter. As there is no X-ray scattering signal indicating a periodic repetition along the column, we cannot determine any precise stacking of the molecules in that direction. Whatever the organization, the projection of the structure on the plane perpendicular to the column presents a hexagonal symmetry (Figure 5).

We looked at the structure factors (Table 3) in terms of the scattering function of a long cylinder of radius R ({2 J1($2\pi Rs$)/$2\pi Rs$ = f($2\pi Rs$)}, where J1 is the first order Bessel function); the experimental structure factors sampled satisfactorily the scattering curve of a cylinder of radius 10.5 ± 1 Å (Figure 4a). This enabled us to give a sign to each reflection (hk) and to compute the corresponding circularly averaged profiles of the electron density, with the assumption of a $p6$ symmetry (Figure 4b). This high-symmetry distribution was chosen to account for the arrangement disorder of the columns. The slope of the electron density decrease from the polar to the paraffinic region was comparable for all the βCD-Cn samples but was smoothest for γCD-C14 (Figure 4). The case of γCD-C14 is particular: well-defined scattering reflections appeared only at high temperature and the corresponding scattering spectrum was characterized by a very strong[10] reflection followed by weak reflections (Table 3, Figure 4); this implies that the scattering elements do not present a very narrow separation in the electron density distribution of γCD-C14 projected orthogonally to the column as revealed by the density profile.

Table 3. Hexagonal Phase: Structure Factors of the (hk) Reflections[a]

	βCD-C6	βCD-C8	βCD-C10	βCD-C12	γCD-C14
	a = 25.9 Å	a = 30.8 Å	a = 33.0 Å	a = 35.3 Å	a = 37.6 Å
hk	F	F	F	F	F
10	331	378	383	377	406
11	185	102	73	90	6
20	128	99	79	116	13
21	40	20	34	92	23
30	26	3	36	76	25
22	29	3	51	39	0
31	28	22	33	20	0

[a] The structure factors are normalized by setting $\Sigma_{(hk)} m_{(hk)} F^2_{(hk)} = 10^6$ where $m_{(hk)}$ is the multiplicity factor of the reflection hk.

A freeze fracture electron microscopy study showed typical images of hexagonal phases with repeating distances in good agreement with the X-ray data. However we encountered difficulties in obtaining freeze fracture surfaces. This was probably because the CD molecules were associated in dimers or trimers which are large with respect to the lattice dimensions. The fracture pathways can thus be found along the hexagonal columns as well as between the groups of CD molecules. These samples can thus behave like crumbly structures.

The Cubic Structure. The experimental results presented above are all consistent with a body-centered cubic structure. The lattice dimension and the molecular volume of the α- or βCD-C14 were used to estimate the number of molecules per unit cell: approximately 12. This value is compatible with several body-centered cubic structures. The possible cubic aspects and their corresponding space groups are Q2 (208), Q4 (201, 224), Q5 (218, 223), Q6 (222), and Q8 (197, 199, 204, 211, 217, 229), and for a set of 12 molecules the possible lattice complexes are $Im3m$(e), $Im3m$(d), $I2_13$(b), and $Im3$, with the point configurations I6z, W*, .3J*2x, and 2_13.SV1z, respectively.[12] However, among all these possibilities, only those that favor the partition of the hydroxyl groups on one hand and of most of the paraffinic chains on the other hand should be considered; this makes the W*, .3J*2x, and 2_13.SV1z configurations unlikely. The most probable lattice complex is $Im3m$(e) with a point configuration I6z ($x00$, $\bar{x}00$, $0x0$, $0\bar{x}0$, $00x$, $00\bar{x}$) at (0,0,0) and ($^1/_2$,$^1/_2$,$^1/_2$). This configuration may also be regarded as formed by six dimers in the $Im3m$(b) lattice complex with the point configuration J* or as formed by two hexamers in the $Im3m$(a) lattice complex with the point configuration I. From the point

(11) Nicolis, I. Systèmes à base de cyclodextrines: physicochimie en milieu ionique; aspects structuraux de nouveaux assemblages, Thesis, Univ Paris VI, 1994.

(12) *International Tables for X-ray Crystallography*; Hahn, T., Ed; Reidel Publishing Co.: Dordrecht, 1983; p A820.

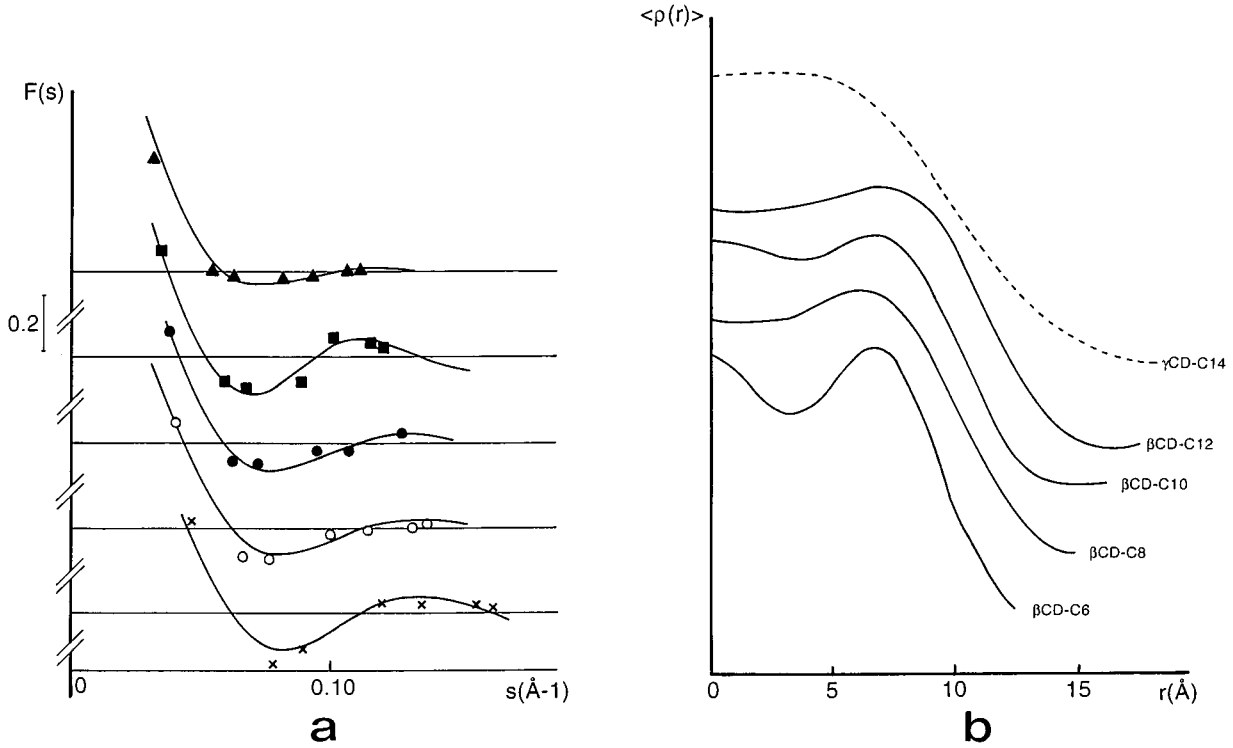

Figure 4. Hexagonal structure factors. (a) The experimental structure factors (×, ○, ●, ■, and ▲, for βCD-C6, -C8, -C10, -C12, and γCDC14) and the curves $\{[J1(2\pi Rs)/(2\pi Rs)]\exp(-\mu^2 s^2)\}$, as a function of s (Å^{-1}); the coefficient μ was used, in some cases, to obtain the best fit: $\mu^2 = 0$, 50, 50, 0, and 200 for βCD-C6, βCD-C8, βCD-C10, βCD-C12, and γCD-C14, respectively. (b) Cylindrical mean electron density $\langle\rho(r)\rangle$ distribution as a function of r(Å).

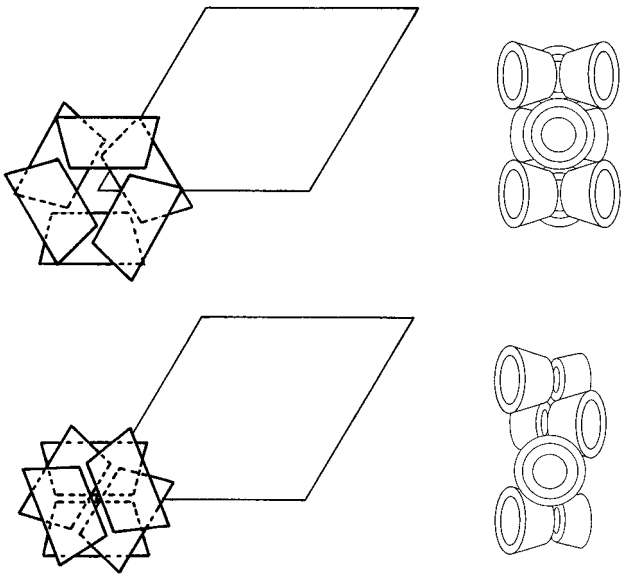

Figure 5. 2D hexagonal structure model. The polar columns consist of piled cyclodextrin moieties. Two possible types of association are drawn; in each case a top and a side view of the column are represented. Due to the presence of fluid paraffin chains, the columns can take any orientation around the direction perpendicular to the 2D lattice.

of view of the polar and hydrocarbon space partition, the proposed structure can be regarded as being formed of two either polar or paraffinic globules located at (0,0,0) and ($^1/_2$,$^1/_2$,$^1/_2$) and thus as corresponding to a $Im3m$(a) lattice complex.

In the first case, each polar globule is formed with six molecules associated through their primary hydroxyl groups and some water molecules, about one per hydroxyl group to fill the space between the polar faces of the molecules (Figure 6, left); this aggregate is surrounded by the paraffinic chains. At a low resolution, the globule can be considered as a spherical particle: indeed the experimental scattering structure factors sampled, in a satisfactory way, the Fourier transform of a sphere of a radius R of about 14 Å (the last term defines a slight apodization that accounts for the limited resolution of the data):

$$F(s) = [\{3\sin(2\pi Rs) - 2\pi Rs\cos(2\pi Rs)\}/(2\pi Rs)^3] \times \exp(-150s^2)$$

The corresponding electron density map was calculated with the assumption of the highest symmetric space group $Im3m$ (229) (Figure 7, left). As the hexagonal structure found in the β series can be considered of the type II (polar columns separated by a hydrophobic region), the cubic structure could plausibly belong to the type II cubic structure, $Im3m$, with a micellar topology. This configuration could be imposed by the paraffin chains: the presence of a polar hexamer can be regarded as a consequence of the existence of dimers formed by the association of the paraffinic regions of the CD molecules. Despite the good agreement between the X-ray data and the model, it is unclear whether the steric constraints imposed by the formation of the polar hexamer could favor such a model.

In the second case, the molecules are associated by their hydroxyl groups to make dimers centered at the middle of each edge of the cubic cell and oriented parallel to the axis of the cubic cell (Figure 6, right). Dimers adjacent on their lateral side are oriented orthogonally to each other. These dimers bring together a large proportion of their paraffinic content to form two hydrophobic micelles, one being located at the center of the cube, the other at its apex. Given the lattice dimension and the height of a CD dimer (about 20 Å), the volume of the two micelles represents 40% of the paraffin content, the remaining

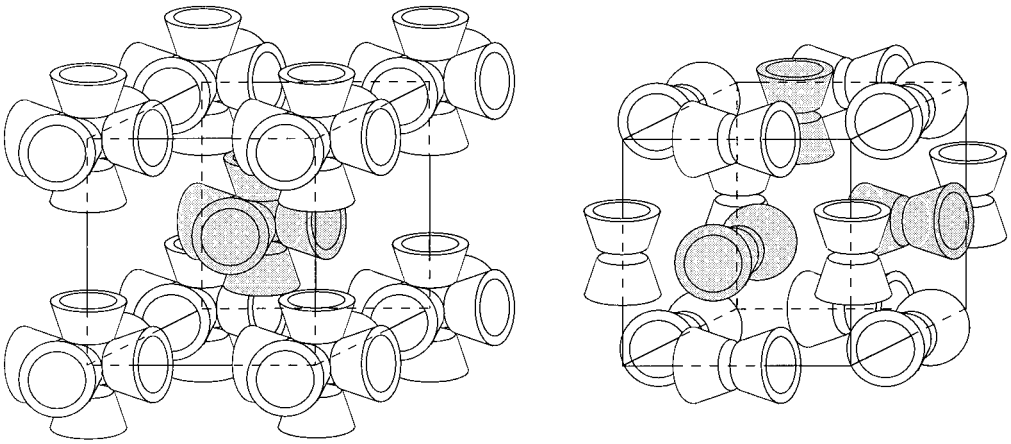

Figure 6. Cubic structure model. 12 molecules are associated in a centered cubic structure. The molecules are aligned along the edges of the cube and are associated into dimers, either through their paraffinic chains or their primary hydroxyl groups. Thus, at the vertex, six molecules form a globule which is either polar (left) or paraffinic (right). The other six molecules are arranged in the same way, with a translation of ($^1/_2$, $^1/_2$, $^1/_2$); for the sake of clarity, only a few of them are drawn and appear in gray tint. For the same reason, the paraffinic chains are not shown.

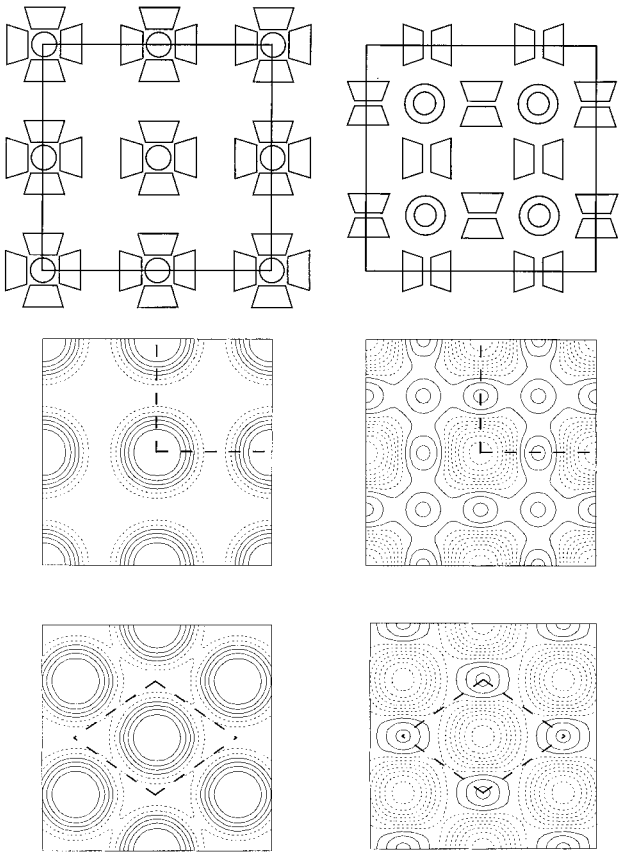

Figure 7. Electron density maps: left, the polar globule model; right, the paraffin globule model. First row, a schematic view of the face of the cube. Second and third rows, the electron density sections for the planes [100] and [110] at the origin. The signs of the structure factors used for the calculation were $+ + - - -$ (left) and $- + - + +$ (right). The density levels represent the normalized electron density fluctuations and are equally spaced from negative (dotted lines) to positive (continuous lines) values with an increment 0.5. The corresponding 2-D lattices are represented by a square and a lozenge (drawn in bold broken lines).

chains fill the space around the lateral side of the CD moiety between adjacent dimers, that is about 5% for one CD molecule. Calculation of the scattering is not simple, because only a part of the paraffinic content is in the globules. Therefore all the possible sign combinations of the structure factors were generated and the electron density maps were determined in the Q229 space group. Several combinations were found to be compatible with the proposed model: the electron density map corresponding to the most satisfying one is represented in Figure 7 (right).

Freeze fracture electron microscopy combined with image processing is a powerful tool which has been successfully used for the structural analysis of several cubic lipidic phases, namely, *Ia*3*d* (Q230), *Fm*3*m* (Q225), *Pn*3*m* (Q223), and *Fd*3*m* (Q227).[9,13−16] This approach first reveals the presence of symmetry elements in the different crystallographic orientations of the fracture planes, which allows the determination of the correct space group among all the possibilities. Second, it also provides faithful information on the shape and distribution of the structure elements. In the present study, we encountered difficulties in visualizing well-preserved ordered fracture domains of CD-C14. This is mainly due to the small lattice dimension but also probably to the spatial molecular arrangement which does not facilitate the propagation of the fracture. A thorough inspection of the unidirectional micrographs revealed a single orientation for all the fracture domains. As we know from previous studies,[9,15] the fracture preferentially propagates along the most paraffinic planes of the structure and thus along directions that are perpendicular to the most intense X-ray reflections which indeed correspond to the cleavage planes of the structure. Hence it is not surprising that we obtained only one fracture direction as the X-ray diffraction displayed only one intense reflection which is (110) (Table 4). Despite our efforts to obtain an exploitable replica after rotary shadowing, we could only use unidirectional shadowing

(13) Delacroix, H.; Gulik-Krzywicki, T.; Mariani, P.; Luzzati, V. Freeze Fracture electron microscopy of lipid systems. The cubic phase of space group *Pm*3*n*. *J. Mol. Biol.* **1993**, *229*, 526−539.

(14) Delacroix, H.; Gulik-Krzywicki, T.; Mariani, P.; Risler, J. L. Freeze Fracture electron microscopy of lyotropic lipid systems. Quantitative analysis of phases of space group *Ia*3*d*(Q230). *Liq. Cryst.* **1993**, *15*, 605−625.

(15) Delacroix, H.; Gulik-Krzywicki, T.; Seddon, J. M. Freeze Fracture electron microscopy of lyotropic lipid systems. Quantitative analysis of the inverse micellar cubic phase of space group *Fd*3*m* (Q227). *J. Mol. Biol.* **1996**, *258*, 88−103.

(16) Gulik, A.; Delacroix, H.; Kirschner, G.; Luzzati, V. Polymorphism of ganglioside-water systems: a new class of micellar cubic phases. Freeze fracture electron microscopy and X-ray scattering studies. *J. Phys. II* **1995**, *5*, 445−464.

Table 4. Cubic Structure: Structure Factors of the (*hkl*) Reflections[a]

hkl	βCD-C14 *F*	αCD-C14 *F*
110	283	277
200	33	60
211	24	27
220	30	31
310	11	18
222	9	19
321	7	17

[a] The structure factors are normalized by setting $\Sigma_{(hkl)} m_{(hkl)} F^2_{(hkl)} = 10^6$ where $m_{(hkl)}$ is the multiplicity factor of the reflection *hkl*.

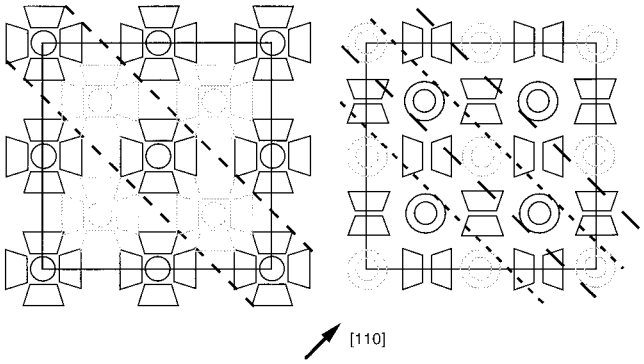

Figure 8. Projection of the possible [110] fracture surfaces in the [100] plane. The [100] view displays the molecules in the plane passing through the origin ($z = 0$); the strippled molecules are located at $z = 1/2$. The projection of the [110] fracture surfaces is indicated by a dotted line. Left frame, for the polar globule model, the two sides of the fracture surface are equivalent and only one aspect is conceivable. Right frame, for the paraffin globule model, two distinct fracture pathways exist (indicated by two different sets of dotted lines); according to the location the fracture surface, the electron micrographs can reveal two distinct aspects, referred to as [110]a and [110]b in the text, as shown in Figure 9.

for further processing. Anyway, image processing performed on unidirectional shadowed replica revealed the presence of two different aspects of subdomains within the [110] fracture domains. These two aspects were not related to each other by simple geometric relationship and thus should correspond to two different parallel fracture pathways through the structure. This observation was essential as it is not compatible with the "polar globule model". Such a structure would provide only one [110] fracture pathway that follows the paraffinic medium between identical layers of globules. Moreover, as the two sides of the fracture are similar, only one fracture aspect could be expected (Figure 8, left). Conversely, in the "paraffin globule model", the paraffin distribution is more complex and can easily account for the existence of two fracture aspects along the [110] direction, [110]a and [110]b. Indeed, there are two possible pathways through the paraffinic medium that separate two distinct layers of dimers (Figure 8, right). In one layer, the symmetry axis of all the molecules is oriented parallel to the [110] plane and in the other, the symmetry axis of the molecules is oriented at −45° or +45° with respect to the [110] plane. The two corresponding fracture surfaces are thus not equivalent and will show distinct features. According to the location of the fracture within the structure, two aspects could therefore appear at the surface of the replica in distinct subdomains of a same domain (Figure 9). This result undoubtedly favors the "paraffin globule model" (Figure 6, right).

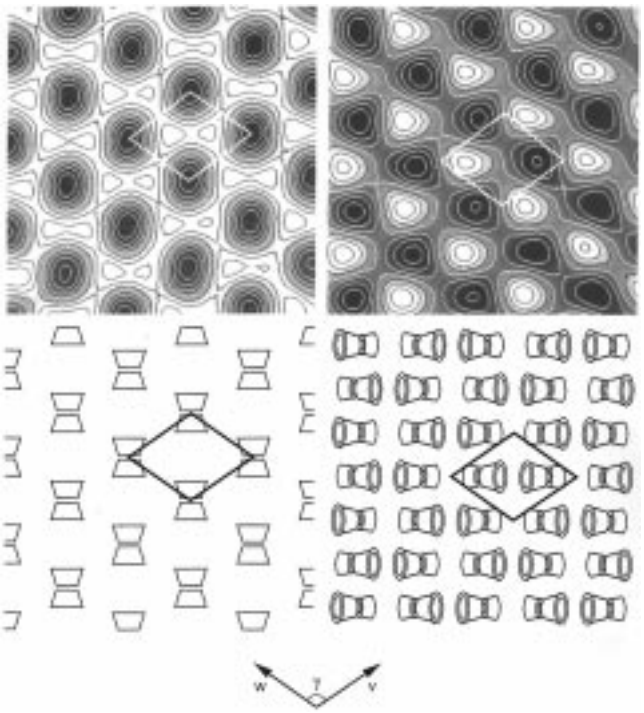

Figure 9. Two freeze fracture aspects. **v**, **w**, and γ indicate the vectors and angle of the periodic lattice in the micrographs (see text). The elements of structure observed on the images obtained after the cross correlation averaging procedure (top) correspond to the location of the molecules in the two possible fracture surfaces (bottom). The occurrence of two aspects, [110]a and [110]b, in the fracture, is compatible with the "paraffin globule model".

Conclusion

We show that amphiphilic cyclodextrins can associate in either hexagonal or cubic crystalline forms. The hexagonal structure consists of polar columns comprising the cyclodextrin moieties and separated by the paraffinic chains. The cubic structure is body centered, and we propose two possible models comprising either a polar or a paraffin aggregate. However the electron microscopic study provides a strong support for the second model. The type of association we reveal is unusual for cyclodextrins and results from the bulkiness of the numerous paraffin chains whose surface area requires a much greater area than the surface area offered by the CD residue. The combination of the two approaches, X-ray scattering and freeze fracture electron microscopy, was useful not only for determining CD structure but also for providing strong arguments for similar structures in the CD nanospheres. The small quantity of water that can be associated with amphiphilic CD may explain the easy formation of cyclodextrin nanospheres by nanoprecipitation, a method widely used for the formation of nanospheres from polymers or copolymers. Generally the internal structure of these nanospheres does not present any internal crystalline organization. In the case of amphiphilic cyclodextrins the nanospheres present an original property, a crystalline internal organization that might have interesting properties of value for drug encapsulation and delivery.

Acknowledgment. We are greatly indebted to A. Coleman for providing the βCD-C10 and γCD-C14 samples. We also greatly appreciate the skillful and technical assistance of J.-C. Dedieu.

LA971019R